

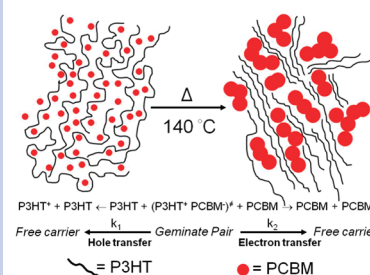
# Dependence of Charge Separation Efficiency on Film Microstructure in Poly(3-hexylthiophene-2,5-diyl):[6,6]-Phenyl-C<sub>61</sub> Butyric Acid Methyl Ester Blend Films

Panagiotis E. Keivanidis,<sup>\*,†</sup> Tracey M. Clarke,<sup>‡</sup> Samuele Lilliu,<sup>§</sup> Tiziano Agostinelli,<sup>†</sup> J. Emyr Macdonald,<sup>§</sup> James R. Durrant,<sup>‡</sup> Donal D. C. Bradley,<sup>†</sup> and Jenny Nelson<sup>\*,†</sup>

<sup>†</sup>Department of Physics, Experimental Solid State Physics Group, The Blackett Laboratory, Imperial College, South Kensington Campus, London SW7 2AZ, U.K., <sup>‡</sup>Department of Chemistry, Imperial College, South Kensington Campus, London SW7 2AZ, U.K., and <sup>§</sup>Department of Physics, University of Cardiff, Queens Buildings, The Parade, Cardiff CF24 3AA, U.K.

**ABSTRACT** Herein we address the factors controlling photocurrent generation in P3HT:PCBM blend films as a function of blend composition and annealing treatment. Absorption, photoluminescence, and transient absorption spectroscopy are used to distinguish the role of exciton dissociation, charge pair separation, and charge collection. Variations in blend film microstructure with composition and annealing treatment are studied using X-ray diffraction. While the trend in photocurrent generation with composition and annealing [Muller, et al., *Adv. Mater.* **2008**, *20*, 3510] does not follow the trend in exciton dissociation, it closely follows the trend in charge pair generation. Moreover, charge pair generation efficiency is positively correlated to the degree of polymer crystallization and the appearance of large domains of both polymer and fullerene phases. We argue that larger domains assist charge pair separation by increasing the probability of escape from the P3HT:PCBM interface, thus reducing geminate charge recombination.

**SECTION** Kinetics, Spectroscopy



Blend films of poly(3-hexylthiophene-2,5-diyl) (P3HT) with [6,6]-phenyl-C<sub>61</sub> butyric acid methyl ester (PCBM) have attracted major attention as a model system for the study of photoinduced charge pair separation and photocurrent generation in organic solar cells. In a polymer:fullerene photovoltaic heterojunction, photocurrent generation results from the following sequence of events: photon absorption in either component of the blend film; migration of the resulting neutral excited electronic state to the polymer–fullerene interface; dissociation of this state to yield a geminate, electrostatically bound charge pair; separation of the geminate pair into free charges, avoiding prompt recombination; and collection of the separated charges at the electrodes, avoiding bimolecular recombination. Each of these stages may be influenced by the blend microstructure, i.e., by the degree of phase segregation and by the order of molecular packing within each phase. The P3HT:PCBM system is particularly interesting in that a high short circuit photocurrent ( $J_{sc}$ ) requires an annealing stage during which polymer crystallization and PCBM aggregation occur, leading to a degree of phase segregation.<sup>1,2</sup> In addition, a strong composition dependence of  $J_{sc}$  is seen.<sup>3</sup> Various mechanisms have been proposed for the specific influence of such microstructural variations on  $J_{sc}$ . Some authors propose that the efficiency of charge pair separation dominates, and is itself controlled either by the size and density of fullerene domains<sup>4</sup>

or by a crystallization-induced change in the driving force for charge separation.<sup>5</sup> Other studies show that annealing results in increased charge mobilities, such that the probability of escaping bimolecular recombination could be increased.<sup>6</sup> Recently, a thermal characterization study<sup>3</sup> of the P3HT:PCBM binary revealed a eutectic phase behavior, whereby the eutectic composition, which corresponds to the maximum interfacial area, is correlated with the composition for maximum  $J_{sc}$ , suggesting an influence of microstructure on the exciton dissociation step. Although it is well-known<sup>7,8</sup> that the efficiency of photocurrent generation in P3HT:PCBM is influenced both by blend composition and by the film microstructure, the specific relationship between film microstructure and charge separation efficiency has not yet been studied in detail. Previous studies on polymer films have addressed the importance of mesoscopic order in charge carrier transport<sup>9</sup> and in the formation of bound charge transfer states.<sup>10</sup> In the present study we address the impact of supramolecular order in the bulk of P3HT:PCBM films on the efficiency of photoinduced charge pair generation.

For our study, we employ time-integrated photoluminescence (PL), steady-state ultraviolet–visible (UV–vis), and

**Received Date:** November 20, 2009

**Accepted Date:** January 21, 2010

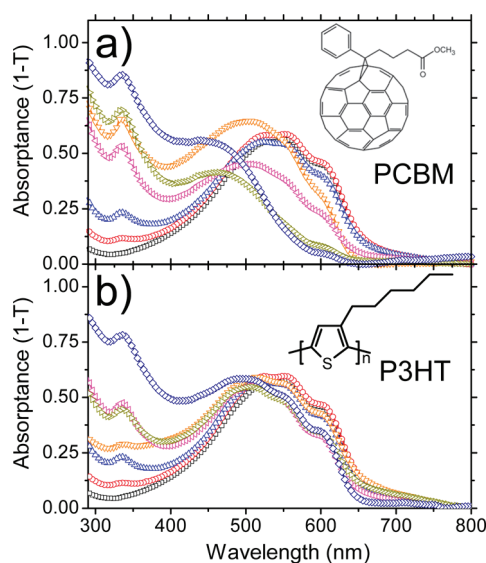


**Figure 1.** UV-vis absorbance spectra of (a) as-spun and (b) annealed films of P3HT:PCBM blends with increasing PCBM content: 0 wt % (black squares), 10 wt % (red circles), 25 wt % (blue up-triangles), 40 wt % (orange down-triangles), 50 wt % (magenta right-tilted triangles), 60 wt % (dark yellow left-tilted triangles), 70 wt % (navy diamonds). The absorbance has been zeroed at the long wavelength regime for eliminating scattering effects.

transient absorption (TA) spectroscopies in order to study the effects of blend composition and blend film microstructure on the efficiency of photoinduced charge pair separation in P3HT:PCBM blend films. For each composition, the degree of crystallinity is varied by blend ratio regulation and thermal annealing of the blend films. The resulting dependence of charge generation on composition and annealing are discussed in terms of the mechanisms listed above.<sup>3,5</sup> X-ray diffraction (XRD) measurements are used to provide additional information on the annealing-induced structural changes that we infer from the spectroscopic studies. Figure 1 presents the UV-vis absorption spectra of as-spun (Figure 1a) and annealed (Figure 1b) P3HT:PCBM films. The degree of structural order in P3HT is associated with the absorption oscillator strength at 610 nm,<sup>11</sup> a feature that is attributed to interchain excitonic coupling.<sup>12,13</sup> Within this context we can conclude that, for the as-spun films, a high degree of order in P3HT chain packing persists when the P3HT content exceeds 70 wt %. For as-spun films of lower P3HT content, the 610 nm absorption is weaker, and the absorption spectrum appears less structured, indicating the amorphous character of the polymeric matrix. As Figure 1b depicts, the crystallinity of the P3HT in the amorphous P3HT:PCBM blends is restored after thermal treatment. Melt processing of the as-spun films showed identical composition-dependent absorption behavior.

Charge photogeneration in bulk heterojunction organic photovoltaic blends results from exciton dissociation via photoinduced charge transfer between the components of the blends. The study of PL quenching is helpful in estimating the efficiency of exciton dissociation in these systems and it can also provide information on the upper limit of the charge photogeneration yield. We have measured the steady-state PL spectra of the prepared P3HT:PCBM films in ambient

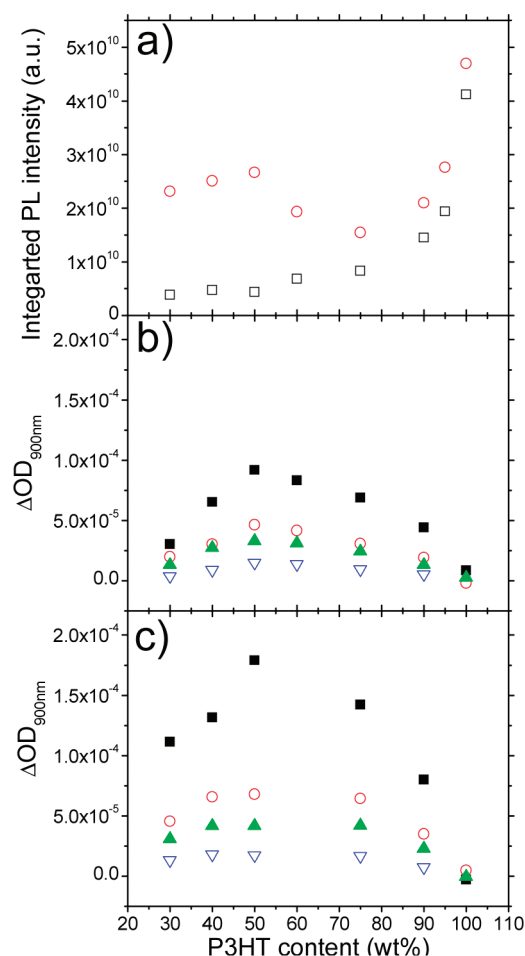


**Figure 2.** The composition dependence of (a) the spectrally integrated (590–755 nm) PL intensity of as-spun (open squares) and annealed (open circles) films of P3HT:PCBM and the TA amplitude at 900 nm of (b) as-spun and (c) annealed films of P3HT:PCBM blends at 1  $\mu$ s (solid squares), 10  $\mu$ s (open circles), 30  $\mu$ s (solid up-triangles) and 300  $\mu$ s (open down triangles). All data points are corrected for absorbance of the films on the excitation wavelength of 510 nm.

conditions. The PL spectra of as-spun and annealed P3HT:PCBM films after photoexcitation at 510 nm are shown in the Supporting Information. Figure 2a depicts the spectrally integrated (590–755 nm) PL intensities for the as-spun and annealed blend films, normalized with respect to the film absorbance (where absorbance =  $1 - T$ , with  $T$  corresponding to transmittance) at the excitation wavelength ( $\lambda_{\text{exc}} = 510$  nm, where light is mainly absorbed by the polymer). We assume that at this spectral range the monitored PL signal is dominated by the luminescence of P3HT without the contribution of any PCBM emission. No differences were found in the trends of Figure 2a when spectral integration was between 640 and 696 nm, the spectral region in which P3HT alone emits.

For the as-spun films a monotonic reduction was observed in the PL intensity of the P3HT band with decreasing P3HT content. In the case of the annealed films, the PL intensity was found to reduce monotonically down to P3HT contents of 75 wt % and then to rise again at lower P3HT contents.

Comparing the PL intensity for as-spun and annealed films, we observe a recovery in PL upon annealing at low P3HT contents, in accordance with previous studies of 50 wt % blend films.<sup>5,14</sup> This effect is most pronounced at those compositions where annealing has the largest effect on P3HT crystallinity. However, it may not be a result of crystallization: previous studies of P3HT polymers of different regioregularity (RR) have shown that higher crystallization (associated with higher RR) tends to reduce PL intensity,<sup>12</sup> probably through the crystallization-induced enhancement of nonradiative pathways for exciton decay. An additional factor influencing nonradiative exciton decay channels may be annealing-induced changes in the concentration of a charge transfer complex associated with the P3HT:PCBM interface, which has been inferred from suboptical gap absorption in P3HT:PCBM blend films.<sup>15</sup>

Next we address the composition and annealing dependence of the charge photogeneration yield. For this purpose we measure the TA signal of these films after excitation at  $\lambda_{\text{exc}} = 510$  nm and probe the excited-state absorption at  $\lambda_{\text{abs}} = 900$  nm, where the P3HT cation is known to absorb on the nanosecond to millisecond time scale.<sup>16</sup> Previous studies showed that the shape of the TA spectrum was unchanged during decay, and was unchanged by annealing.<sup>5</sup> The amplitude of the TA signal,  $\Delta\text{OD}$ , at a given time delay after excitation is thus always proportional to the concentration of the P3HT polaron at that time. Figures 2b and 2c depict  $\Delta\text{OD}$  (normalized with respect to the absorbance at the excitation wavelength) at various times after excitation as a function of P3HT content for as-spun and annealed films. In contrast to the monotonic decrease of the P3HT PL intensity with decreasing P3HT content,  $\Delta\text{OD}$ , and hence the charge generation yield, is maximized at a P3HT:PCBM blend ratio of approximately 50 wt % for both as-spun and annealed films.

The observed decrease in  $\Delta\text{OD}$  and increase in PL intensities at high P3HT content is consistent with a decrease in the volume of P3HT adjacent to PCBM domains, within which exciton dissociation could occur. This is supported by the trend seen in our XRD measurements (see in Supporting Information), where P3HT domains increase in size with reducing PCBM content and with annealing. At low P3HT content, however,  $\Delta\text{OD}$  is not well correlated to the PL for either as-spun or annealed films. In particular,  $\Delta\text{OD}$  increases upon annealing, while PL also increases. This confirms the previous observation that PL quenching is not quantitatively linked to charge generation yield in photovoltaic blends such as P3HT:PCBM.<sup>7,16</sup> In a polymer of low PL quantum efficiency such as P3HT, charge photogeneration competes with other, nonradiative exciton decay pathways usually involving inter-chain interactions.<sup>13</sup> Since these interactions tend to increase upon crystallization such that PL would be expected to decrease, another mechanism must be responsible for the observed increase in PL upon annealing. Most likely, this is the enlargement of pure domains of each phase through molecular reorganization and crystallization during annealing (see XRD data in Supporting Information). The thermally equilibrated microstructure of the P3HT:PCBM binary corresponds to a eutectic phase behavior and so the departure of a well-mixed, PCBM rich blend from this equilibrium is expected to

reduce the interfacial area available for exciton dissociation. Note that the concentration at which PL quenching is greatest after annealing ( $\sim 75$  wt % P3HT) corresponds roughly to the eutectic composition ( $\sim 65$  wt % P3HT) at which the interfacial area is maximized.<sup>3</sup> Given that, on the microsecond time scale, PL quenching is a poor indicator of charge separation, we now address the relationship between  $\Delta\text{OD}$  and  $J_{\text{sc}}$ .  $\Delta\text{OD}$  can be interpreted as a measure of the photoinduced charge density that escapes prompt (geminate) recombination. The photocurrent generation efficiency is a measure of the product of the efficiencies of exciton dissociation, geminate pair separation, and carrier collection (survival of bimolecular recombination). The  $J_{\text{sc}}$  measured in as-spun and annealed P3HT:PCBM devices, as a function of the PCBM content, is presented in ref 3. (Figure 2a of that reference). The close correlation between the optimum  $\Delta\text{OD}$  and optimum  $J_{\text{sc}}$ , which both occur at  $\sim 50$  wt % after annealing,<sup>3</sup> indicates that the efficiency of geminate pair separation is a significant factor influencing short-circuit photocurrent generation, especially for annealed P3HT:PCBM blend films. (In the case of as-spun blend films, the disruptive effect of PCBM on the P3HT crystallinity, and hence on hole mobility,<sup>6</sup> may cause bimolecular recombination losses at low P3HT content. This effect shifts the composition needed for high  $J_{\text{sc}}$  to higher P3HT content than for the annealed case.) The correlation between  $\Delta\text{OD}$  and  $J_{\text{sc}}$  suggests that TAS could be used as a predictive tool for device performance.

We now address the mechanism controlling the optimization of the charge generation yield. The results presented above for the composition and annealing dependence of  $\Delta\text{OD}$  indicate that  $\Delta\text{OD}$  is positively correlated with large interfacial area (as expected) and with polymer crystallinity. However, if these two factors alone controlled  $\Delta\text{OD}$ , then the optimum composition after annealing might be expected to lie at the eutectic composition of  $\sim 65$  % P3HT, where interfacial area is maximized. Instead,  $\Delta\text{OD}$  is maximized at a more PCBM-rich content (50 % P3HT). In agreement with previous microscopic studies<sup>17</sup> our PL studies above show that higher PCBM content leads to growth of PCBM aggregates; therefore the presence of these domains appears to assist the separation of geminate charge pairs. This could occur, for instance, by improved electronic coupling between the vibrationally hot geminate pair state and the polaron states in the larger or better packed fullerene domains. A similar mechanism has been proposed previously for fluorene copolymer:fullerene blend films.<sup>4</sup> The present studies support that conclusion regarding the case of P3HT:PCBM blend films. We note that an additional effect of annealing may be a crystallization-induced shift in charge separation energetics, as we have discussed elsewhere.<sup>5</sup>

The TA data we have recorded for high photoexcitation light intensities (see Supporting Information) suggest that, while the  $\Delta\text{OD}$  at short times ( $< 1$   $\mu\text{s}$ ) can be interpreted mainly in terms of survival of geminate recombination, the decay dynamics over longer time scales ( $> 1$   $\mu\text{s}$ ) provide information about the nongeminate trap-limited charge recombination dynamics. Recent experimental and theoretical work has addressed the process of bimolecular recombination in polymer-based donor–acceptor blend devices.<sup>18–20</sup> In



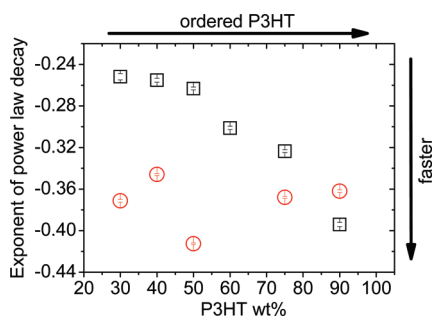


**Figure 3.** The power-law exponents of the TA decay monitoring bimolecular recombination of the studied as-spun (squares) and annealed (circles) films of P3HT:PCBM blends.

accordance with previous analyses,<sup>21</sup> power law decays were chosen to fit the dynamics of the TA signal. The power law was rationalized<sup>22</sup> by invoking the presence of an exponential tail of sites within the energetic density of states of the hole-transporting component. Figure 3 depicts the composition dependence of the exponent obtained from such a fitting procedure for the as-spun and the annealed films.

For the as-spun films at low P3HT content, the dynamics are slow (small negative exponent). This can be explained by noting that for such films the P3HT is relatively amorphous and contains structural traps, leading to slow carrier transport and slow bimolecular recombination kinetics. At high P3HT content, the P3HT matrix is more crystalline, leading to fewer deep charge traps and therefore to faster transport of photo-induced carriers, as evident in the larger negative exponent.<sup>6</sup> After annealing, the P3HT crystallinity is high at all compositions (as indicated in Figure 1), leading to relatively fast transport and bimolecular recombination and to a relatively large negative exponent in all cases. The similar decay dynamics for all compositions after annealing implies a weak composition dependence of bimolecular recombination. This is completely consistent with the observation above that the maximum  $\Delta OD$  coincides with the maximum  $J_{sc}$ , i.e., for annealed films, exciton dissociation and survival of geminate recombination are the dominant factors at short circuit. The herein-presented TA data are thus in agreement with recent reports on increased hole mobility of P3HT due to ordering effects<sup>23</sup> and suggest the contribution of a high degree of order in the bulk of the blend components to the dynamics of charged states in the photoactive layer.

In conclusion, we have addressed the dependence of free charge photogeneration efficiency on film microstructure in P3HT:PCBM photovoltaic films, using blend film composition and annealing treatment as a means to regulate microstructure. Our spectroscopic investigation in conjunction with structural studies have shown that photogeneration yield in P3HT:PCBM films is positively correlated not only with interfacial area and with polymer crystallinity but also with domain size.

**SUPPORTING INFORMATION AVAILABLE** Experimental methods, grazing incidence XRD data of in situ annealed P3HT:PCBM blends, composition-dependent absorbance at 510 nm and PL spectra of as-spun and annealed P3HT:PCBM films, and high photoexcitation density TA transients of as-spun P3HT:PCBM films.

This material is available free of charge via the Internet at <http://pubs.acs.org>.

## AUTHOR INFORMATION

### Corresponding Author:

\*To whom correspondence should be addressed. E-mail: [pekeivan@imperial.ac.uk](mailto:pekeivan@imperial.ac.uk) (P.E.K.); [jenny.nelson@imperial.ac.uk](mailto:jenny.nelson@imperial.ac.uk) (J.N.).

**ACKNOWLEDGMENT** We acknowledge Merck Chemicals for the kind provision of the P3HT material used in this study and BP Solar for financial support. We thank Dr. A. Ballantyne for useful discussions.

## REFERENCES

- (1) Li, G.; Shrotriya, V.; Huang, J.; Yao, Y.; Moriarty, T.; Emery, K.; Yang, Y. High-Efficiency Solution Processable Polymer Photovoltaic Cells by Self-Organization of Polymer Blends. *Nat. Mater.* **2005**, *4*, 864–868.
- (2) Campoy-Quiles, M.; Ferenczi, T.; Agostinelli, T.; Etchegoin, P. G.; Kim, Y.; Anthopoulos, T. D.; Stavrinou, P. N.; Bradley, D. D. C.; Nelson, J. Morphology Evolution via Self-Organization and Lateral and Vertical Diffusion in Polymer:Fullerene Solar Cell Blends. *Nat. Mater.* **2008**, *7*, 158–164.
- (3) Muller, C.; Ferenczi, T. A. M.; Campoy-Quiles, M.; Frost, J. M.; Bradley, D. D. C.; Smith, P.; Stingelin-Stutzmann, N.; Nelson, J. Binary Organic Photovoltaic Blends: A Simple Rationale for Optimum Compositions. *Adv. Mater.* **2008**, *20*, 3510–3515.
- (4) Veldman, D.; Ipek, O.; Mesker, S. C. J.; Sweelssen, J.; Koetse, M. M.; Veenstra, S. C.; Kroon, J. M.; van Bavel, S. S.; Loos, J.; Janssen, R. A. J. Compositional and Electric Field Dependence of the Dissociation of Charge Transfer Excitons in Alternating Polyfluorene Copolymer/Fullerene Blends. *J. Am. Chem. Soc.* **2008**, *130*, 7221–7235.
- (5) Clarke, T. M.; Ballantyne, A. M.; Nelson, J.; Bradley, D. D. C.; Durrant, J. R. Free Energy Control of Charge Photogeneration in Polythiophene/Fullerene Solar Cells: The Influence of Thermal Annealing on P3HT/PCBM Blends. *Adv. Funct. Mater.* **2008**, *18*, 4029–4035.
- (6) Mihailescu, V. D.; Xie, H.; de Boer, B.; Koster, L. J. A.; Blom, P. W. M. Charge Transport and Photocurrent Generation in Poly(3-hexylthiophene):Methanofullerene Bulk Heterojunction. *Solar Cells. Adv. Funct. Mater.* **2006**, *16*, 699–708.
- (7) Kim, Y.; Cook, S.; Tuladhar, S. M.; Choulis, S. A.; Nelson, J.; Durrant, J. R.; Bradley, D. D. C.; Giles, M.; McCulloch, I.; Ha, C.-S.; Ree, M. A Strong Regioregularity Effect in Self-Organizing Conjugated Polymer Films and High-Efficiency Polythiophene:Fullerene Solar Cells. *Nat. Mater.* **2006**, *5*, 197–203.
- (8) Moule, A. J.; Bonekamp, J. B.; Meerholz, K. The Effect of Active Layer Thickness and Composition on the Performance of Bulk-Heterojunction Solar Cells. *J. Appl. Phys.* **2006**, *100*, 094503(1)–094503(7).
- (9) Wegner, G.; Ruhe, J. The Structural Background of Charge-Carrier Motion in Conducting Polymers. *Faraday Discuss. Chem. Soc.* **1989**, *88*, 333–349.
- (10) Hallermann, M.; Krieger, I.; Da Como, E.; Berger, J. M.; von Hauff, E.; Feldmann, J. Charge Transfer Excitons in Polymer/Fullerene Blends: The Role of Morphology and Polymer Chain Conformation. *Adv. Funct. Mater.* **2009**, *19*, 3662–3668.
- (11) Zen, A.; Pflaum, J.; Hirschmann, S.; Zhuang, W.; Jaiser, F.; Asawapirom, U.; Rabe, J. P.; Scherf, U.; Neher, D. Effect of

- 344 Molecular Weight and Annealing of Poly(3-hexylthiophene)s  
345 on the Performance of Organic Field-Effect Transistors. *Adv.*  
346 *Funct. Mater.* **2004**, *14*, 757–764.
- 347 (12) Xu, B.; Holdcroft, S. Molecular Control of Luminescence from  
348 Poly(3-hexylthiophenes). *Macromolecules* **1993**, *26*, 4457–  
349 4460.
- 350 (13) Clark, J.; Silva, C.; Friend, R. H.; Spano, F. C. Role of Inter-  
351 molecular Coupling in the Photophysics of Disordered Or-  
352 ganic Semiconductors: Aggregate Emission in Regioregular  
353 Polythiophene. *Phys. Rev. Lett.* **2007**, *98*, 206406(1)–  
354 206406(4).
- 355 (14) Ayzner, A. L.; Wanger, D. D.; Tassone, C. J.; Tolbert, S. H.;  
356 Schwartz, B. J. Room to Improve Conjugated Polymer-Based  
357 Solar Cells: Understanding How Thermal Annealing Affects  
358 the Fullerene Component of a Bulk Heterojunction Photo-  
359 voltaic Device. *J. Phys. Chem. C* **2008**, *112*, 18711–18716.
- 360 (15) Goris, L.; Poruba, A.; Hod'áková, L.; Vanecek, M.; Haenen, K.;  
361 Nesládek, M.; Haenen, K.; Nesladek, M.; Wagner, P.; Vander-  
362 zande, D.; De Schepper, L.; Manca, J. V. Observation of the  
363 Subgap Optical Absorption in Polymer–Fullerene Blend  
364 Solar Cells. *Appl. Phys. Lett.* **2006**, *88*, 052113(1)–052113(3).
- 365 (16) Ohkita, H.; Cook, S.; Astuti, Y.; Duffy, W.; Tierney, S.; Zhang,  
366 W.; Heeney, M.; McCulloch, I.; Nelson, J.; Bradley, D. D. C.;  
367 Durrant, J. R. Charge Carrier Formation in Polythiophene/  
368 Fullerene Blend Films Studied by Transient Absorption Spec-  
369 troscopy. *J. Am. Chem. Soc.* **2008**, *130*, 3030–3042.
- 370 (17) Swinnen, A.; Haeldermans, I.; Ven, v. M.; D'Haen, J.; Vanhoy-  
371 land, G.; Aresu, S.; D'Olieslaeger, M.; Manca, J. Tuning the  
372 Dimensions of C<sub>60</sub>-Based Needlelike Crystals in Blended Thin  
373 Films. *Adv. Funct. Mater.* **2006**, *16*, 760–765.
- 374 (18) Deibel, C.; Baumann, A.; Dyakonov, V. Polaron Recombina-  
375 tion in Pristine and Annealed Bulk Heterojunction Solar Cells.  
376 *Appl. Phys. Lett.* **2008**, *93*, 163303(1)–163303(3).
- 377 (19) Shuttle, C. G.; O'Regan, B.; Ballantyne, A. M.; Nelson, J.;  
378 Bradley, D. D. C.; Durrant, J. R. Bimolecular Recombination  
379 Losses in Polythiophene:Fullerene Solar Cells. *Phys. Rev. B*  
380 **2008**, *78*, 113201(1)–113201(4).
- 381 (20) Groves, C.; Greenham, N. C. Bimolecular Recombination in  
382 Polymer Electronic Devices. *Phys. Rev. B* **2008**, *78*,  
383 155205(1)–155205(8).
- 384 (21) Nogueira, A. F.; Montanari, I.; Nelson, J.; Durrant, J. R.;  
385 Winder, C.; Sariciftci, N. S.; Brabec, C. Charge Recombination  
386 in Conjugated Polymer/Fullerene Blended Films Studied by  
387 Transient Absorption Spectroscopy. *J. Phys. Chem. B* **2003**,  
388 *107*, 1567–1573.
- 389 (22) Nelson, J. Diffusion-Limited Recombination in Poly-  
390 mer–Fullerene Blends and Its Influence on Photocurrent  
391 Collection. *Phys. Rev. B* **2003**, *67*, 155209(1)–155209(10).
- 392 (23) McNeill, C. R.; Halls, J. J. M.; Wilson, R.; Whiting, G. L.;  
393 Berkebile, S.; Ramsey, M. G.; Friend, R. H.; Greenham, N. C.  
394 Efficient Polythiophene/Polyfluorene Copolymer Bulk Het-  
395 erojunction Photovoltaic Devices: Device Physics and An-  
396 nealing Effects. *Adv. Funct. Mater.* **2008**, *18*, 2309–2321.